# Preparation for an Emittance Exchange Based Bunch Compression Experiment at Argonne Wakefield Accelerator Facility


Jimin Seok
*Department of Physics*
*UNIST*
Ulsan, Korea
linker123@unist.ac.kr

Gwanghui Ha
*High Energy Physics*
*Argonne National Laboratory*
Chicago, USA
gha@anl.gov

John Gorham Power
*High Energy Physics*
*Argonne National Laboratory*
Chicago, USA
JP@anl.gov

Manoel Conde
*High Energy Physics*
*Argonne National Laboratory*
Chicago, USA
conde@anl.gov

Moses Chung
*Department of Physics*
*UNIST*
Ulsan, Korea
mchung@unist.ac.kr



***Abstract*— The emittance exchange (EEX) is a recently developed beam manipulation method providing the longitudinal bunch compression. Since EEX converts the transverse phase space to the longitudinal phase space, it can generate a sub-fs bunch when a small bunch gets appropriate transverse focusing. Argonne Wakefield Accelerator facility (AWA) plans to demonstrate this EEX based sub-fs generation for the high frequency wakefield acceleration. The primary experiment is planned in this summer to explore the minimum achievable bunch length of current configuration. The result will indicate what upgrades we need to experimentally generate a sub-fs bunch. We present progress on the simulation work for this summer experiment and modified EEX beamline generating the sub-fs bunch as an example.**



***Keywords—simulation work, emittance exchange, bunch compression, sub-fs, AWA***


## I. Introduction

Generation of a short electron bunch (fs) has gained increasing attention in the accelerator community. This short bunch can preserve its high beam quality in high frequency wakefield accelerators [1,2], and provides a high resolution to observe the instantaneous changes of structures in ultrafast electron diffraction (UED) [3-4]. Since electron bunch's temporal property characterizes X-ray's temporal property, it plays a key role for the time-resolved experiment using X-ray free electron lasers (XFELs) [5]. While these short bunches have been successfully generated by the magnetic compression [6,7], the stage is moved from fs to the sub-fs level to achieve a higher quality and resolution.

Among the methods explored to generate a sub-fs bunch [6-10], we focus on the emittance exchange (EEX)-based bunch compressor in this paper. Since the EEX beamline provides the exchange of transverse and longitudinal phase spaces, it converts transverse focusing to longitudinal compression. Compared to other methods, this EEX-based method does not require any incoming chirp [11] and it can control the chirp out of the beamline [12]. Instead, the bunch length at the downstream of the EEX beamline is proportional to the transverse emittance and the reciprocal of the beam size at the entrance. Transverse manipulation on a low emittance beam can reach sub-fs level with EEX beamline.

In this paper, we present simulation results to show the feasibility of sub-fs bunch generation. Simulations were carried out using ELEGANT [13] including one-dimensional coherent synchrotron radiation (CSR). Since undesired effects such as higher order effects from magnets and thick-cavity effect [14] limit the compression ratio, we suppressed these effects using sextupole magnets and fundamental mode cavity (FMC) [11]. In addition to the feasibility check, we present the simulations to prepare the preliminary experiment planned at Argonne Wakefield Accelerator (AWA). This preliminary experiment plans to find the minimum bunch length from the current configuration and sources limiting to achieve a sub-fs bunch. Longitudinal chirp, horizontal slope and horizontal beam size are scanned during the simulation. These scan results provide the effects of higher order, thick cavity and CSR on the final bunch length.

## II. Princple of EEX Bunch Compression

Fig. 1 depicts process of bunch compression using the EEX beamline. Quadrupole before the EEX beamline applies a transverse focusing to the beam, and the EEX beamline converts this focusing to the longitudinal compression via emittance exchange process. Rest of section present details of this compression. We assume a zero-length deflecting cavity (TDC) in this section to simplify the discussion while the rest of paper uses a TDC with a finite length [15, 17].

When the 4D particle coordinate is $X = (x, x', z, \delta)^T$, the beam transport through the beamline can be described as,

$$X_f = RX_i, \tag{1}$$

where subscripts i and f correspond to the entrance and the exit to the beamline, and $R$ is the transfer matrix. When R is the transfer matrix of the EEX beamline, longitudinal position of the particle at the exit ($z_f$) is expressed as,

$$z_f = \kappa\xi x_i + (\eta + \kappa\xi L)x'_i, \tag{2}$$


Work supported by the National Research Foundation of Korea (Grant No. NRF-2015R1D1A1A01061074) and Department of Energy, Office of Science (No. DE-AC02-06CH11357)



978-1-5386-7721-6/18/$31.00 ©2018 IEEE

where $\kappa$ is normalized TDC kick strength, $\xi$ and $\eta$ are the momentum compaction factor and the dispersion of the dogleg, L is the summation of particle travel distance along the dogleg and the distance between dipole and TDC. Eq. (2) can be extended to second moment, and the transverse terms on the right-hand side can be minimized when the horizontal slope ($\sigma_{xx'}/\sigma^2_x$) satisfies,

$$\sigma_{xx'}/\sigma^2_x = -\kappa\xi/(\eta+\kappa\xi L). \quad (3)$$

The minimum bunch length can be expressed as,

$$\sigma_{z,f} = (\eta+\kappa\xi L)\varepsilon_{x,i}/\sigma_{x,i}, \quad (4)$$

where $\varepsilon_{x,i}$ is rms horizontal emittance and $\sigma_{x,i}$ is rms horizontal beam size at the entrance to the EEX beamline.

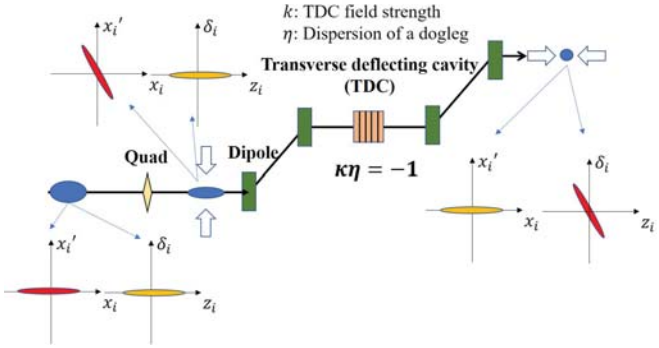


Fig. 1: Schematic to show EEX bunch compression mechanism.

## III. Feasibility of Sub-fs Bunch Compression

### A. Suppression of Undesired Effects

Among all undesired effects, we focus on thick cavity effect and higher order effects in the EEX beamline [14]. Under the lengthening from these two effects, the longitudinal position of particles at the exit ($z_f$) can be expressed as,

$$z_f = R_{51}x_i+R_{52}x'_i+R_{55}z_i+R_{56}\delta_i+T_{511}x_i^2+T_{522}x'^2_i, \quad (5)$$

where $R_{5m}$ and $T_{5nn}$ are linear and second order terms in the transfer matrix of the EEX beamline. Other second order terms are negligible. Compared to the Eq. (2), $z_f$ have extra terms from initial longitudinal phase space ($R_{55}z_i$ and $R_{56}\delta_i$) due to the thick-cavity effect and dependency on $x_i^2$ and $x'^2_i$ from second order effects.

Fig. 2 shows ELEGANT simulation to observe the cure of the thick-cavity effect and the second order effect by means of FMC and sextupole magnets. In Fig. 2a, the final longitudinal phase space is spread and curved. The spread feature is originated from the thick-cavity effect (indicated by the arrow) while the curved feature is originated from the second order effect (indicated by the white curve).

When FMC is added to the beamline, it eliminates the acceleration term from TDC, and the phase space becomes narrow (see Fig. 2b). Similarly, second order effect is suppressed by sextupole magnets. The white curve in Fig. 2a shows quadratic trend since it is originated from $T_{511}$ and $T_{522}$ of the EEX beamline and have quadratic dependency on initial x and x'. When sextupole magnets decrease these terms, this quadratic tendency disappears from the longitudinal phase space as shown in Fig. 2c. Finally, when both FMC and three sextupole magnets are added to the beamline as Fig. 3, the thick-cavity effect and the second order effect are suppressed as shown in Fig. 4d.

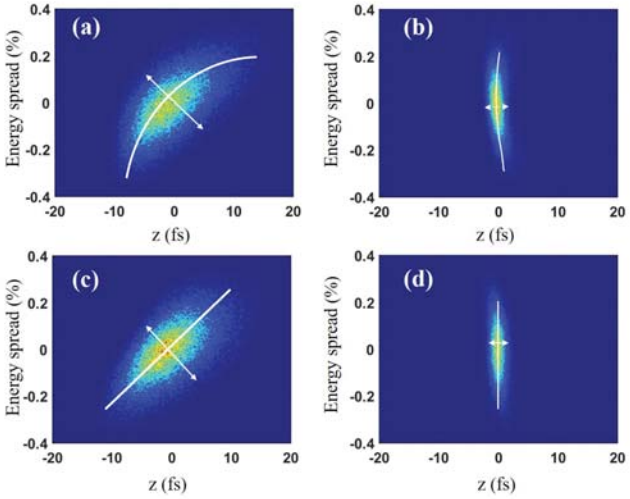


Fig. 2: (a) is the longitudinal phase spaces without any correction. White arrow and curve indicate the thick-cavity effect and the second order effect, respectively. (b) and (c) are the longitudinal phase space with the correction on the thick-cavity effect and second order effect respectively. Corrections on both effects are applied for (d).

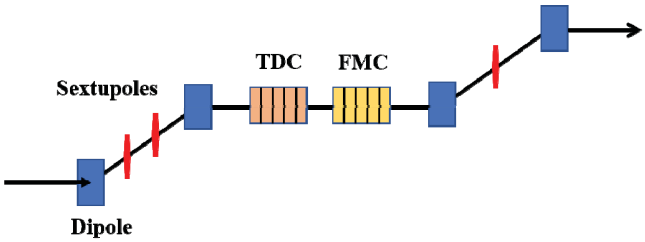


Fig. 3: Configuration of an EEX beamline to generate a sub-fs bunch. Three sextupole magnets and an FMC are added to the beamline to suppress the thick-cavity effect and the second order effects on the bunch compression.

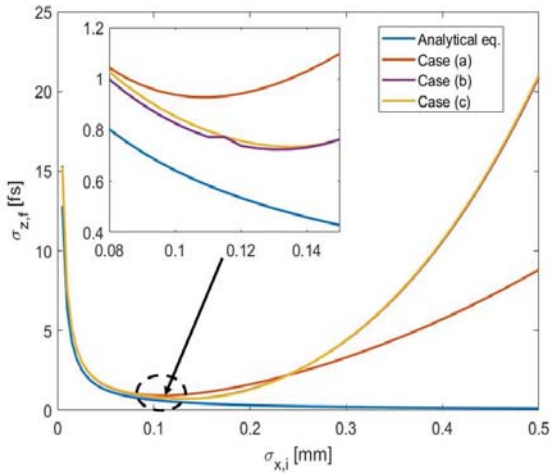


Fig. 4: Final bunch length is simulated with different initial horizontal beam size. The blue curve is calculated from analytical equation which is based on the linear transfer matrix with a thin TDC. Case (a), (b) and (c) are ELEGANT simulation results. (a) shows the bunch length without any correction and CSR effect. (b) shows the result with sextupole correction but CSR is still ignored. CSR effect is applied for the case (c).

### *B. Simulation Results for sub-fs Bunch Generation*

Fig. 3 shows the configuration of the EEX beamline used in the simulation. Three sextupole magnets are located on the diagonal of doglegs, and an FMC is placed next to the TDC. 6D Gaussian beam was used for the simulation and its energy and charge are 100 MeV and 2 pC, respectively.

Three different cases are simulated to observe the changes from undesired effects and their correction. Eq. (4) provides a bunch length at the end of the beamline and it is shown in Fig. 4 (blue) as function of initial horizontal beam size. Since this is based on a linear transport of the beam, Elegant simulation result with second order effect (case a) shows different trend than the blue curve. A large beam size at the entrance is supposed to provide a short bunch length at the end in the linear transport system. However, $T_{511}$ term increases as the beam size increases, and the final bunch length from the initial beam size larger than 0.1 mm grows up and it shows a quadratic trend.

Case (b) in Fig. 4 shows the result with sextupole magnets and FMC to cure the second order effect and thick-cavity effect. Here the sextupole magnets are optimized to $\sigma_{xi}$=0.1 mm, so the bunch length near this area is shorter than the bunch length from Case (a) but it becomes quadratic again after this area. Case (c) shows the results with CSR effect, and it does not show significant differences due to a low charge (2 pC) and low angle (5˚) in this simulation.

The bunch length at the exit including all physics is 0.90 fs when $\sigma_{xi}$ is 0.1 mm. As shown in Fig. 4, it can be further compressed to 0.72 fs with a larger beam size ($\sigma_{xi}$=0.14 mm).

## IV. Simulations for Preliminary Experiment at AWA

AWA [18] plans to demonstrate the sub-fs bunch generation for high frequency wakefield accelerator application. This sub-fs bunch will preserve its high beam quality in the high frequency wakefield acceleration.

As the first step, preliminarily experiment is planned to find the minimum bunch length from the current configuration [18]. At the same time, the experiment will explore limiting factors. Fig. 5 shows the current beamline configuration. The charge of 200 pC will be accelerated to 48 MeV with the gun and 4 linac tanks.

Since the current beamline does not have sextupole magnets and FMC, second order effects and thick-cavity effect should be strong enough to limit an achievable bunch length. At the same time, a large bending angle of a dogleg (20˚) would introduce a strong CSR effect on the compression process. These effects are strongly related to the three beam properties; horizontal beam size, horizontal slope, and longitudinal chirp. We plan to scan these parameters to observe the limiting effects during the experiment. The longitudinal chirp will be controlled by adjusting the linac phase, and horizontal properties will be manipulated with four quadrupoles in front of the EEX beamline.

Based on the experiment plan, OPAL-T [19] code simulated the final bunch length with various incident beam conditions. All cavity phases are moved together so that the linac phase has a simple relation with the chirp. Quadrupole strengths are found by Genetic Algorithm, and the beam size and the slope are set to the objective.

Fig. 6 shows OPAL simulation results, and blue and red curves correspond to CSR off and on cases respectively. One of the parameters is scanned while other parameters are fixed to the reference values. The reference value for the beam size, the slope, and the phase are 0.8 mm, -1.6 $m^{-1}$, -14˚.

When CSR is not applied to the simulation, the linac phase of -14˚ minimizes the bunch length (see Fig. 6a). A different phase generates a stronger thick-cavity effect, and it results in a longer bunch length. However, the CSR effect changes the trend here. The chirp condition minimizing the thick-cavity effect is also the condition to minimize the bunch length in the middle of the EEX beamline [20]. It generates a strong CSR and increases the bunch length at the end. Therefore, the linac phase minimizing the bunch length is shifted closer to 0˚ when CSR is applied to the simulation.

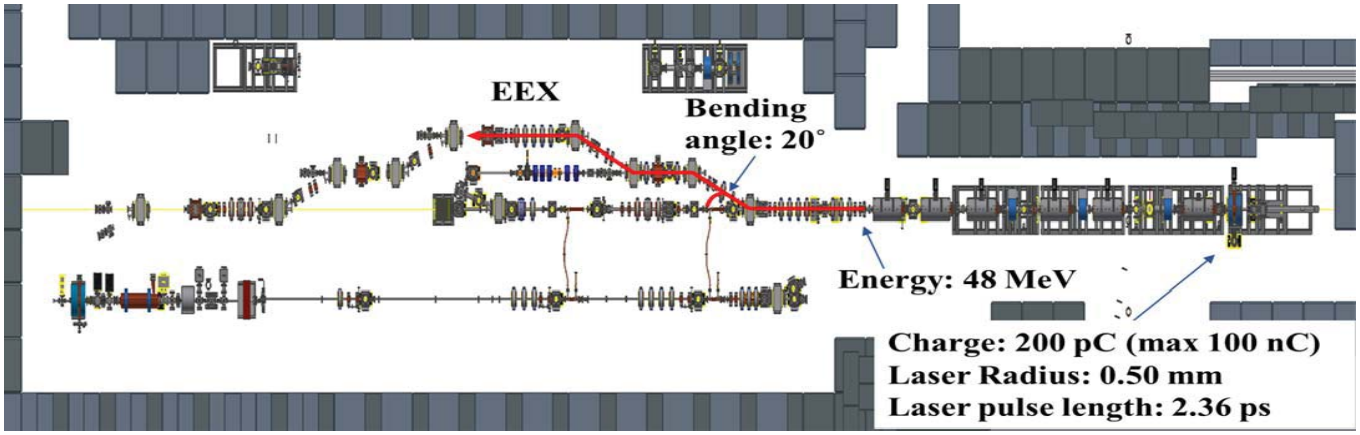


Fig. 5. Layout of Argonne Wakefield Accelerator. The red line indicates the path to the EEX beamline. Four quadrupoles are located in front of the EEX beamline to manipulate transverse properties of incident beam.

The slope of -1.6 $m^{-1}$ is supposed to minimize the bunch length according to the linear transport. However, the real minimum from the simulation is around -1.45 $m^{-1}$ as shown in Fig. 6b. In this configuration, the slope condition to minimize the bunch length in the first order and the second order are not matched. These two terms make another balanced value to minimize the total bunch length. Except for the shift of minimizing slope, the bunch length is quadratic to the slope due to the second order effects. Due to a similar reason, the minimizing slope under CSR shifts again. The chirp of -14˚, the slope of -1.6 $m^{-1}$ and the beam size of 0.9 mm provides the minimum bunch length in the current configuration.

Fig. 7 shows longitudinal phase spaces before (left) and after (right) the EEX beamline with the minimum bunch length conditions. The minimum bunch length is 15 μm (=50 fs), and it is compressed from the initial 645 μm (=215 fs). This bunch length is apparently longer than the target bunch length (sub-fs) due to the lengthening from undesired effects (higher order, thick cavity and CSR). Fig. 6 shows the second order effect and the CSR effect in the EEX beamline are dominant limiting factors. Sextupole magnets and appropriate CSR suppression are necessary to achieve below 15 μm.

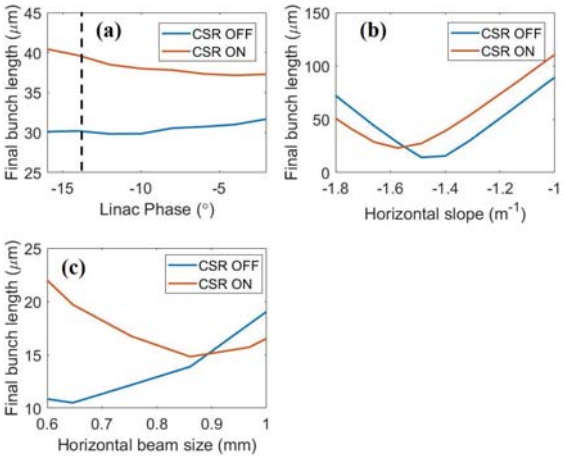


Fig. 6. Final bunch length scanning results. CSR is off for blue curves and it is on for orange curves. The reference values for the beam size, the slope and the chirp are 0.8 m, -1.6 $m^{-1}$, and -14 ˚, and one of them are scanned while others are fixed.

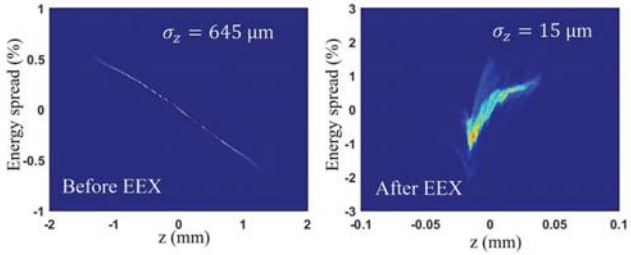


Fig. 7. Initial (left) and final (right) longitudinal phase space, respectively
.

## V. Conclusions

We achieved a sub-fs bunch length from the ELEGANT simulation of the EEX beamline. When sextupole magnets and an FMC are applied to the modified EEX beamline, it successfully reduces the second order effect and the thick-cavity effect. Since the beam size and the emittance introduce an intrinsic limit, the beam size at the entrance should be increased to compress the bunch further. In this case, sextupole magnet may not be enough to suppress the higher order effects, and higher order magnet such as octupole magnet might be required to suppress it.

Preliminary experiment in this summer aims to find the minimum bunch length from the current configuration and the limiting factors of the compression. OPAL simulation expects the minimum bunch length of 15 μm from the current beamline installed at AWA. We found the second order effects dominantly limit the bunch compression, sextupole magnets are necessary to achieve below 15 μm. Also, CSR is another significant effect to consider due to a large bending angle of the AWA EEX beamline.

## References

[1] B. D. O'Shea, et al., "Observation of acceleration and deceleration in gigaelectron-volt-per-metre gradient dielectric wakefield accelerators," Nat. Commun., vol. 7, 2016. [online]. Available: https://doi.org/10.1038/ncomms12763.

[2] J.B. Rosenzweig G. Travish, M. Hogan, and P. Muggli, "High frequency, high gradient dielectric wakefield accelerator experiments at SLAC and BNL," SLAC, Menlo Park, CA, USA, Report No. SLAC-PUB-15153, 2010. [online]. Available: http://www.slac.stanford.edu/cgi-wrap/getdoc/slac-pub-15153.pdf.

[3] S. Chen, M. T. Seidel, and A. H. Zewail, “Atomic-scale dynamical structures of fatty acid bilayers observed by ultrafast electron crystallography,” Proc. Natl. Acad. Sci., vol. 102, no. 25, pp. 8854–8859, June 2005. [online]. Available: https://doi.org/10.1073/pnas.0504022102.

[4] E. Fill, L. Veisz, A. Apolonski, and F. Krausz, “Sub-fs electron pulses for ultrafast electron diffraction,” New J. Phys., vol. 8, November 2006. [online]. Available: http://iopscience.iop.org/article/10.1088/1367-2630/8/11/272/meta.

[5] J. B. Rosenzweig, et al., “Generation of ultra-short, high brightness electron beams for single-spike SASE FEL operation,” Nucl. Instrum. Methods Phys. Res., Sect. A, vol. 593, pp. 39–44, August 2008.

[6] B. Marchetti et al., “Electron-beam manipulation techniques in the SINBAD Linac for external injection in plasma wake-field acceleration,” Nucl. Instrum. Methods Phys. Res., Sect. A, vol. 829, pp. 278–283, September 2016.

[7] J. Zhu, R. W. Assmann, M. Dohlus, U. Dorda, and B. Marchetti, “Sub-fs electron bunch generation with sub-10-fs bunch arrival-time jitter via bunch slicing in a magnetic chicane,” Phys. Rev. Accel. Beams, vol. 19, no. 5, p. 054401, May 2016. [online]. Available: https://link.aps.org/doi/10.1103/PhysRevAccelBeams.19.054401.

[8] K. Floettmann, “Generation of sub-fs electron beams at few-MeV energies,” Nucl. Instrum. Methods Phys. Res., Sect. A, vol. 740, pp. 34–38, March 2014.

[9] M. J. H. Luttikhof, A. G. Khachatryan, F. A. Van Goor, and K. J. Boller, “Generating ultrarelativistic attosecond electron bunches with laser wakefield accelerators,” Phys. Rev. Lett., vol. 105, no. 12, p. 124801, September 2010.

[10] J.M. Seok, G. Ha, J.G. Power, M. Conde, and M. Chung., “Sub-fs electron bunch generation using emittance exchange compressor,” proceedings of the 9th International Particle Accelerator Conference, IPAC’18, Vancouver, BC, Candata, April 30 - May 4, 2018. pp. 1501-1503. [online]. Available: JACow, http://www.jacow.org/.

[11] A.A.Zholents, and M.S. Zolotorev, “A new type of bunch compressor and seeding of a short wave length coherent radiation,” ANL, Chicago, IL, USA, Report No. ANL-APS-LS-327, May 2011. [online]. Available: https://www.aps.anl.gov/files/APS-sync/lsnotes/files/APS_1421246.pdf.

[12] G. Ha, J.G. Power, M. Conde, D.S. Doran, and W. Gai, “ Prelimunarily simulations on chirp-less bunch compression using double-EEX beamline,” Proceedings of 8th International Particle Accelerator Conference, IPAC’17, Copenhagen, Denmark, May 14-19, 2017. pp. 3862-3864. [online]. Available: JACow, http://www.jacow.org/.

[13] ops.aps.anl.gov/manuals/elegant_latest/elegant.html

[14] G. Ha, M. H. Cho, W. Gai, K. J. Kim, W. Namkung, and J. G. Power, “Perturbation-minimized triangular bunch for high-transformer ratio using a double dogleg emittance exchange beam line,” Phys. Rev. Accel. Beams, vol. 19, no. 12, p. 121301, December 2016. [online]. Available: https://link.aps.org/doi/10.1103/PhysRevAccelBeams.19.121301.

[15] M. Cornacchia and P. Emma, “Transverse to longitudinal emittance exchange,” Phys. Rev. Spec. Top. Accel. Beams, vol. 5, no. 8, p. 084001, August 2002. [online]. Available: https://link.aps.org/doi/10.1103/PhysRevSTAB.5.084001.

[16] P. Emma, Z. Huang, K.-J. Kim, and P. Piot, “Transverse-to-longitudinal emittance exchange to improve performance of high-gain free-electron lasers,” Phys. Rev. Spec. Top. Accel. Beams, vol. 9, no. 10, p. 100702, October 2006. [online]. Available: https://link.aps.org/doi/10.1103/PhysRevSTAB.9.100702.

[17] Y. E. Sun, et al., “Tunable subpicosecond electron-bunch-train generation using a transverse-to-longitudinal phase-space exchange technique,” Phys. Rev. Lett., vol. 105, no. 23, p. 234801, December 2010.

[18] M. E. Conde et al., “Research program and recent results at the Argonne wakefield accelerator facility (AWA),” proceedings of the 8th International Particle Accelerator Conference, IPAC’17, Copenhagen, Denmark, 2017. pp. 2885-2887. [online]. Available: JACow, http://www.jacow.org/.

[19] gitlab.psi.ch/OPAL/src/wikis/home.

[20] J. C. T. Thangaraj, et al., “Experimental studies on coherent synchrotron radiation at an emittance exchange beam line,” Phys. Rev. Spec. Top. Accel. Beams, vol. 110702, p. 110702, November 2012. [online]. Available: https://link.aps.org/doi/10.1103/PhysRevSTAB.15.110702.